

Spontaneous Polarization, Spin Current and Quantum Vortices in Exciton-Polariton Condensates

Bo Xiong^{1,2}

¹*Department of Physics, Nanchang University, 330031 Nanchang, China*

²*Skolkovo Institute of Science and Technology, Novaya Street 100, Skolkovo 143025, Russian Federation*

(Dated: January 10, 2017)

We show that how to support propagation of spin degree in a spin-symmetric exciton-polariton condensates in a semiconductor microcavity. Due to the stimulated spin-dependent scattering between hot excitons and condensates, exciton polaritons form a circular polarized condensate with spontaneous breaking the spin rotation symmetry. The spin antiferromagnetic state are developed evidently from the density and spin flow pumped by localized laser source. The low energy spin current is identified where the steady state is characterized by the oscillating spin pattern. We predict via simulation that it is very promising to dynamical creation of fractionalized half-quantum vortices induced by effective non-abelian gauge potential within currently experiment procedure.

PACS numbers: 72.25.Rb, 75.30.Ds, 72.70.+m, 71.36.+c

I. INTRODUCTION.

Recently, in semiconductor microcavities with quantum wells sandwiched between highly reflective mirrors, the strong coupling is achieved between excitons and photons [1–4]. Such coherent light-matter particles called exciton-polaritons obey the Bose-Einstein statistics and thus condense at critical temperatures ranging from tens Kelvin [5–7] till several hundreds Kelvin [8, 9], which exceeds by many orders of magnitude the Bose-Einstein condensation temperature in atomic gases. Recently, electrically pumped polariton laser or condensation was realized based on a microcavity containing multiple quantum wells [10, 11]. Considering the high transition temperatures and high tunability from pumping source, semiconductor microcavities are perfectly suited for studies of macroscopically collective phenomenon and have initiated the fascinating research on the polariton quantum hydrodynamics.

The polaritons have two allowed spin projections on the structure growth axis, ± 1 , corresponding to right- and left- circular polarizations of photons. In diverse semiconductor materials like GaAs/GaAlAs [12], Si [13], organic single-crystal microcavity $\text{SiN}_x/\text{SiO}_2$ [14] and so on, spin injection and detection has been successfully realized which is one of the key ingredients for functional spintronics devices. A number of prominent spin-related phenomena both in interacting and in noninteracting polariton systems have already been predicted and observed in the microcavities, such as, spontaneous polarization [15–19], polarization multistability [20–22], optical spin Hall effect [23–29] and topological insulator [30, 31].

Spin degrees of freedom in two-dimensional exciton-polaritons superfluid can drastically change elementary topological vortices referred to as half-quantum vortices (HQV) [32–36] which are characterized by a half-integer value of vorticity in contrast to the regular quantum vortex [37, 38, 40, 41] where the vorticity takes only integer values. Usually HQV carry only one half-integer topological charge originating from the superfluid current proportional to $\nabla\theta$ and due to the π spin disclinations superimposed with half-vortices as a result of Berry's phases induced by spin rotations [42]. Similar half vortices have been discussed in A phase of ^3He [43–45] or in triplet

superconductors Sr_2RuO_4 [46] or spinor atomic Bose-Einstein condensates [47–50], described as having two or more superfluid condensates with different spin states and the HQV is then a vortex in just one of them [51–55].

In this paper, we study spontaneous polarization under nonlocal spin injection in a weakly interacting gas of exciton-polariton condensates. We find a dramatically enhanced spin-polarized signal at the appropriate pumping regime when taking into account incoherent hot exciton reservoir scattered into coherent states. The coherent spin antiferromagnetic state is also identified which reveals spin injection and spin current that can be manipulated by spin rotation symmetric pumping source, and may open up new ways of thinking about spintronic devices. Finally, we find direct ways for the dynamic generation of fractionalized HQV around which spin currents circulate as a result of Berry's phases induced by spin rotations.

II. PHYSICAL BACKGROUND.

In the absence of external magnetic field the “spin-up” and “spin-down” states $\sigma = \pm$ of noninteracting polaritons, or their linearly polarized superpositions, are degenerate corresponding to the right (σ_+) and left (σ_-) circular polarizations of external photons. The spinor nature of exciton polaritons can therefore be manifested since the spin of the exciton polaritons are essentially free in semiconductor microcavities. To illustrate the fully degenerate spinor nature, and as a first step, to reach a good approximation of this case, the Zeeman energy must be much smaller than the interaction energy, thus we shall consider only the case of zero magnetic field. Since the interaction between two exciton polaritons depends on their total spins (singlet or triplet), the spin states of the exciton polaritons can be changed after the scattering. The spin-dependent interactions cause the polariton spin states exchange. Moreover, additional mixing may come from the longitudinal-transverse (LT) splitting of polaritons (referred to as the Maialle mechanism) [56] and from structural anisotropies [57].

The low energy dynamics of the system is therefore described by a pairwise interaction that is rotationally in-

variant in the spin space and preserves the spin of the individual exciton polaritons. The general form of this interaction is $\hat{V}(\mathbf{r}_1 - \mathbf{r}_2) = \delta(\mathbf{r}_1 - \mathbf{r}_2) \sum_{F=0}^{2f} g_F \cdot \hat{P}_F$ where $g_F = 4\pi\hbar^2 a_F / M$, M is the mass of exciton polaritons, \hat{P}_F is the projection operator which projects the pair 1 and 2 into a total spin F state, and a_F is the s-wave scattering length in the total spin F channel. For exciton polaritons of $f = 1$ bosons, we have $\hat{V} = g_0 \cdot \hat{P}_0 + g_2 \cdot \hat{P}_2$. In terms of nonlinear optics, the coupling coefficients of polarization independent c_0 and so-called linear-circular dichroism c_2 can be estimated through the matrix elements of the polariton-polariton scattering in the singlet and triplet configurations.

It is convenient to write the Bose condensate $\Psi_a(\mathbf{r}) \equiv \langle \hat{\psi}_a(\mathbf{r}) \rangle$ as $\Psi_a(\mathbf{r}) = \sqrt{n(\mathbf{r})} \zeta_a(\mathbf{r})$, where $n(\mathbf{r})$ is the density, and ζ_a is a normalized spinor $\zeta^+ \cdot \zeta = 1$. It is obvious that all spinors related to each other by gauge transformation $e^{i\theta}$ and spin rotations $\mathcal{U}(\alpha, \beta, \gamma) = e^{-iS_x\alpha} e^{-iS_y\beta} e^{-iS_z\gamma}$ are degenerate, where (α, β, γ) are the Euler angles.

The non-equilibrium dynamics of polariton condensates is described by a Gross-Pitaevskii type equation for the coherent polariton field, which should be coupled to a reservoir of hot excitons that are excited by the nonresonant exciting pump. The model is, however, generalized to take into account the polarization degree of freedom of hot exciton. In this approach, instead of polarization independent scattering, we must take into account dichroism scattering between hot exciton and coherent polariton field.

Let us turn to the pseudospin representation, then the local spin density \vec{s} at the position \mathbf{r} and time t is $\vec{s}(\mathbf{r}, t) = \Psi^\dagger(\mathbf{r}, t) \vec{\sigma} \Psi(\mathbf{r}, t)$, where $\vec{\sigma} = (\hbar/2) \hat{\sigma}$ with $\hat{\sigma}$ being the Pauli matrices. The usual definition of the free-particle probability current $\mathbf{J}_n = \text{Re} \left[\Psi^\dagger(\mathbf{r}, t) \frac{\hat{\mathbf{p}}}{m} \Psi(\mathbf{r}, t) \right]$, where \hat{I} is the identity, and probability spin current $\mathbf{J}_{\vec{s}} = \text{Re} \left[\Psi^\dagger(\mathbf{r}, t) \frac{\hat{\mathbf{p}}}{m} \vec{\sigma} \Psi(\mathbf{r}, t) \right]$. The emergent magnetic monopoles are defined by analogy with Maxwell's equation as $\nabla \cdot \vec{s}$ characterized by a divergent in-plane pseudospin pattern which is present in other systems, such as magnetically frustrated materials or spin-ice [58–64] such as magnetic nanowires [65] and atomic spinor Bose-Einstein condensates [66, 67]. The dynamics of each spin in a magnetic field is governed by the precession equation $\partial_t \mathbf{S} = \mathbf{H} \times \mathbf{S} / \hbar$. The total effective magnetic field \mathbf{H}

represents the sum of the field responsible provided by the spin dependent and independent polariton-polariton interactions and polariton-hot exciton interaction (LT splitting \mathbf{H}_{LT} is assumed to be negligible in high density regime). Very different from those isolated or closed system, the dynamic of spin pattern in such open-dissipative system is crucially determined by the pump source. We will go into further details in the following.

III. THEORETICAL MODEL.

In the following, we study the propagation of polarized polariton in the a planar microcavity and generation of spin injection, spin current and the observability of the HQV, in realistic structures. The equation of motion for

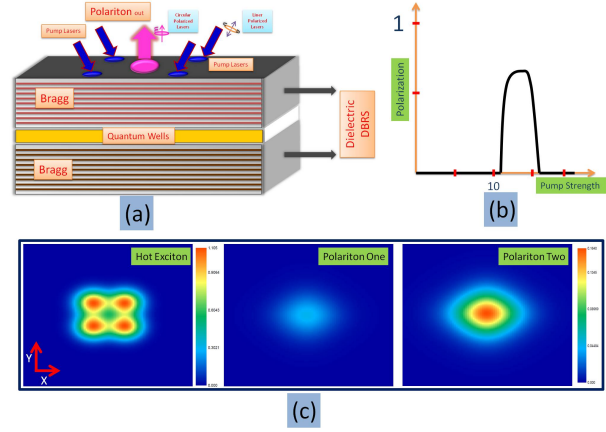


Figure 1: (Color online) The spontaneously circular polarization of spinor condensate non-resonantly pumped by linearly polarized laser. (a) Proposed scheme to experimentally stimulating spontaneous circular polarization by nonpolarized laser beam. (b) Spinor is polarized when the laser power is larger than one threshold value, however, unpolarized after laser power is above second threshold value. (c) Density distribution of hot exciton (left picture which is the same profile for both components) and spinor polariton (middle and right pictures for each components) in real space. Here, simulations in the absence of disorder for four pumping points with a small radius $1.54 \mu\text{m}$. The values of the parameters used in the simulations are shown in the paper.

the spinor polariton wave function reads [68–71]

$$i\hbar\partial_t\psi_{\pm}(\mathbf{r}) = \left\{ -\frac{\hbar^2}{2m}\nabla^2 + \frac{i\hbar}{2}(g_2n_{R\pm} + h_2n_{R\mp} + \beta_2|\psi_{\pm}|^2 + f_2|\psi_{\mp}|^2 - \gamma_C) + V_{ext}(\mathbf{r}) \right\} \psi_{\pm}(\mathbf{r}) \\ + \{ \hbar(\beta_1|\psi_{\pm}|^2 + f_1|\psi_{\mp}|^2) + V_R(\mathbf{r}) \} \psi_{\pm}(\mathbf{r}), \quad (1)$$

where ψ_{σ} represents the condensed field, with $\sigma = \pm$ representing the spin state of polaritons with effective mass m . γ_C represents the coherent polariton decay rate. β_1 and f_1 is the spin-conserved and spin-exchange polariton-polariton interaction strength, respectively. $n_{R\sigma}$ is the

density of the incoherent hot exciton reservoir. And here, $V_R(\mathbf{r}) = \hbar[g_1n_{R\pm} + h_1n_{R\mp} + \Omega P_{\pm}(\mathbf{r})]$ represents the reservoir produces spin-conserved and spin-exchange interactions where $P_{\pm}(\mathbf{r})$ is the spatially dependent pumping rate and $g_1, h_1, \Omega > 0$ are phenomenological coef-

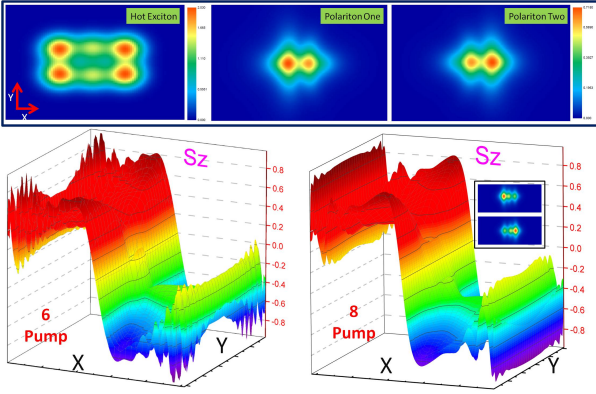


Figure 2: (Color online) The spontaneously circular polarization of spinor condensate non-resonantly pumped by 6 and 8 linearly polarized laser, respectively. Top panel: density distribution of hot exciton (left picture which is the same profile for both components) and spinor polariton (middle and right pictures for each components) in real space for 6 pumping points. Bottom panel: distribution of magnetic polarization along the Z axis for 6 pumping points (left picture) and 8 pumping points (right picture, inset shows density distribution of two component polariton). The values of the parameters used in the simulations are the same as those in the Fig. 1.

ficients to be determined experimentally. $V_{ext}(\mathbf{r})$ represents the static disorder potential typical in semiconductor microcavities, which is chosen as the same for both component polaritons. $g_2 n_{R\pm}$ and $h_2 n_{R\mp}$ is related to the condensation rate, representing the process where hot excitons with same spin or cross spin are stimulated growth of condensate, respectively. [72]. β_2 and f_2 are the same-spin and cross-spin nonradiative loss rates, respectively.

The equation 1 for the condensate is coupled to a rate equation for the evolution of the incoherent hot exciton density $n_{R\sigma}$ which is given by the rate equation:

$$\partial_t n_{R\pm} = -\Gamma n_{R\pm} - [g_2 |\psi_{\pm}|^2 + h_2 |\psi_{\mp}|^2] n_{R\pm} + P_{\pm}, \quad (2)$$

where the reservoir relaxation rate Γ is much faster $\Gamma \gg \gamma_C$ under the Gaussian pump laser $P_{\pm} = W$ which is assumed nonpolarized (corresponding to linear or horizontal polarization through the paper), giving a sufficient large occupation in momentum space of incoherent hot exciton. The stimulated emission of the hot exciton reservoir into the two-component condensate mode is taken into account by the term $[g_2 |\psi_{\pm}|^2 + h_2 |\psi_{\mp}|^2] n_{R\pm}$. The spatial diffusion rate of reservoir density has been neglected. In the following, we solve the coupled Eqs. 1 and 2 numerically starting from a small random initial condition, then, the time evolution of the system can be calculated until a steady state is reached which is independent of the initial noise.

IV. STEADY STATE.

A. Spatially homogeneous system

Let us begin with some analytical consideration on finding spinor condensate. In the homogeneous case, i.e.,

under a spatially homogeneous pumping and in the absence of any external potential, Eqs. 1 and 2 admit analytical stationary spinor configuration. Below the pumping threshold, the condensate remains unpopulated, while the reservoir grows linearly with the pump intensity $n_{R\pm} = W/\Gamma$. At the threshold pump intensity W^{th} , the stimulated emission rate exactly compensates the losses $g_2 n_{R\pm} + h_2 n_{R\mp} = \gamma_C$ and condensate becomes populated dynamically. We notice that threshold pump intensity becomes $W^{th} = \Gamma \gamma_C / (g_2 + h_2)$. Above the threshold, the reservoir density is homogeneous $n_{R\pm} = W / (\Gamma + g_2 |\psi_{\pm}|^2 + h_2 |\psi_{\mp}|^2)$, from this, we obtain

$$Z_R \sim -\frac{W(g_2 - h_2)}{\Gamma^2 + \Gamma(g_2 + h_2)n_c} Z_C, \quad (3)$$

here, we have defined reservoir polarization $Z_R = n_{R+} - n_{R-}$, condensate polarization $Z_C = |\psi_+|^2 - |\psi_-|^2$ and condensate total density $n_c = |\psi_+|^2 + |\psi_-|^2$. As long as $g_2 \neq h_2$, condensate polarization is directly proportional to the reservoir polarization. From the Eqs. 1, we find that the condensate density grows as

$$n_c \sim \frac{(W - W^{th})}{\gamma_C} \cdot \frac{1}{1 - \frac{1}{2} \left(\frac{W}{W^{th}} + \frac{\beta_2 + f_2}{g_2 + h_2} \frac{\Gamma}{\gamma_C} \right)}, \quad (4)$$

and condensate polarization

$$M_C Z_C = 0. \quad (5)$$

where

$$M_C = \left(4Wg_2h_2 + \Gamma^2(\beta_2 - f_2) - \frac{W\Gamma^2\gamma_C^2}{W^{th} \cdot W^{th}} \right).$$

The Eq. 5 has solution for the magnetization of condensate $Z_C = 0$ except very stringent condition $M_C = 0$. Specially, if assuming cross-spin radiative and nonradiative loss rates is negligible. we find laser power should satisfy

$$W = \frac{\gamma_C^2}{\beta_2 (W^{th})^2} = \frac{g_2^2}{\beta_2 \Gamma^2}, \quad (6)$$

then, from necessary condition $W > W^{th}$, in order to spontaneous magnetization, we find

$$\frac{g_2^3}{\beta_2 \gamma_C \Gamma^3} > 1,$$

should be complied.

If assuming condensate wave function takes the form $\psi_{\pm}(\mathbf{r}) = \sum \psi_{\mathbf{k}_{\pm}\omega_{\pm}} e^{i(\mathbf{k}_{\pm} \cdot \mathbf{r} - \omega_{\pm}t)} \sim \psi_{0\pm} e^{i(\mathbf{k}_{\pm} \cdot \mathbf{r} - \omega_{\pm}t)}$, we find spectrum of spinor condensate is given by

$$\omega_{\pm} = \frac{\hbar k_{\pm}^2}{2m} + \tilde{\Omega}_{\pm} W, \quad (7)$$

where

$$\begin{aligned} \tilde{\Omega}_{\pm} = & \Omega + \frac{(\beta_1 + f_1)n_c \pm (\beta_1 - f_1)Z_C}{2W} \\ & + \frac{2(g_1 + h_1)\Gamma + G \cdot n_c \pm H \cdot Z_C}{2[\Gamma^2 + \Gamma(g_2 + h_2)n_c + A]}, \end{aligned}$$

here, wave vector \mathbf{k}_\pm and frequency ω_\pm remains so far undetermined, and coefficient $G = g_1 g_2 + g_1 h_2 + g_2 h_1 + h_1 h_2$, $H = (g_1 h_2 + g_2 h_1 - g_1 g_2 - h_1 h_2)$. However, from Eq. 7, we find energy difference between two component condensate is

$$\omega_+ - \omega_- = \frac{\hbar(\mathbf{k}_+^2 - \mathbf{k}_-^2)}{2m} + \Delta\tilde{\Omega}, \quad (8)$$

here,

$$\Delta\tilde{\Omega} \sim Z_C \{(\beta_1 - f_1)/W - (g_1 - h_1)(g_2 - h_2)/[\Gamma^2 + \Gamma(g_2 + h_2)n_c + A]\},$$

where A is high order term of density and polarization $A = (g_2 + h_2)^2(n_c^2 + Z_C^2)/4$ which can be dominant term for the larger condensate density and polarization. Interestingly, we can see that energy gap is polarization Z_C dependence and especially, which does not depend on the laser power when $\beta_1 \simeq f_1$ or large enough laser power.

B. Local density and spin approximation

In the presence of an inhomogeneous laser pump $W(\mathbf{r})$ (or multiple pump $W_i(\mathbf{r})$), much richer phenomena will be represented in our system, like, spin domain, magnetic monopole, half vortex and so on. In this case, we can look for stationary spinor polariton wave function of the following form

$$\Psi = \begin{pmatrix} \psi_+ \\ \psi_- \end{pmatrix} = \sqrt{\rho(\mathbf{r})} \zeta(\mathbf{r}) e^{-i(\phi(\mathbf{r}) - \omega_\pm t)}, \quad (9)$$

where $\rho(\mathbf{r})$ and $\phi(\mathbf{r})$ are the local density and phase of the condensate wave function, and $\zeta(\mathbf{r})$ is spinor function. We are going to assume that the local pump imposes a boundary condition for the spinor-function at each pumping spot r_p : $\lim_{r \rightarrow r_p} \zeta(\mathbf{r}) = \lambda$, $\lim_{r \rightarrow r_p} \mathbf{k}_C(\mathbf{r}) = 0$, here, we have defined local condensate density wave vector $\mathbf{k}_C(\mathbf{r}) = \nabla_{\mathbf{r}} \phi(\mathbf{r})$. In what follows, we use the dimensionless form of the model obtained by using the scaling units of time, energy, and length: $T = 1/\gamma_C$, $E = \hbar\gamma_C$, $L = \sqrt{\hbar/m\gamma_C}$. Inserting spinor form Eq. 9 into the Eqs. of motion 1 and 2, one obtains the following set of conditions after considering stationary solution:

$$\omega_\pm = -\frac{1}{2} \left(\frac{\nabla^2 \sqrt{\rho}}{\sqrt{\rho}} + \frac{\nabla^2 \zeta_\pm}{\zeta_\pm} + 2 \frac{\nabla \sqrt{\rho} \cdot \nabla \zeta_\pm}{\sqrt{\rho} \zeta_\pm} - k_C^2 \right) + \frac{1}{\gamma_C} (\beta_1 |\zeta_\pm|^2 \rho + f_1 |\zeta_\mp|^2 \rho + g_1 n_{R\pm} + h_1 n_{R\mp}) + \frac{\Omega W}{\gamma_C}, \quad (10)$$

and

$$\frac{1}{2} (g_2 n_{R\pm} + h_2 n_{R\mp} + \beta_2 |\zeta_\pm|^2 \rho + f_2 |\zeta_\mp|^2 \rho - \gamma_C) + \frac{1}{2} \nabla \cdot \mathbf{k}_C(\mathbf{r}) + \frac{\nabla \sqrt{\rho} \cdot \mathbf{k}_C(\mathbf{r})}{\sqrt{\rho}} + \frac{\mathbf{k}_C(\mathbf{r}) \cdot \nabla \zeta_\pm}{\zeta_\pm} = 0, \quad (11)$$

and

$$\Gamma n_{R\pm} + (g_2 |\zeta_\pm(\mathbf{r})|^2 + h_2 |\zeta_\mp(\mathbf{r})|^2) \rho(\mathbf{r}) n_{R\pm} = W(\mathbf{r}). \quad (12)$$

Different from the single component condensate, now in Eq. 10, the quantum pressure terms are not only originated from density $\nabla^2 \sqrt{\rho}$ but also from the spinor $\nabla^2 \zeta$ and even spin-density coupling $\nabla \sqrt{\rho} \cdot \nabla \zeta$. In particular, in Eq. 11, besides the current divergence term liking in single component condensate, the terms associated with coupling between superfluid current and density pressure $\nabla \sqrt{\rho} \cdot \mathbf{k}_C(\mathbf{r})$ or spin pressure $\mathbf{k}_C(\mathbf{r}) \cdot \nabla \zeta$ are appeared. We can make local density approximation (LDA) and local spin approximation (LSA) if the spatial variation of the laser pump profile $W(\mathbf{r})$ is smooth enough, where the quantum pressure term in Eq. 10 and 11 are neglected. Under these LDA and LSA, similar to the homogeneous case, the condensate density profile and condensate polarization is given by the Eq. 4 and Eq. 5, respectively, with the local value of the laser pump power $W(\mathbf{r})$.

Under the Gaussian laser pump profile, we can look for cylindrically symmetric stationary solutions where the condensate frequency ω_\pm is determined by the boundary condition that the local condensate density wave vector vanishes $\mathbf{k}_C(\mathbf{r} = \mathbf{r}_p) = 0$ at the center of the each pumping spot, i.e.,

$$\omega_\pm = \frac{\tilde{\Omega}_\pm \cdot W}{\gamma_C}, \quad (13)$$

where

$$\tilde{\Omega}_\pm = \Omega + \frac{(\beta_1 + f_1) \rho \pm (\beta_1 - f_1) \rho S_Z}{2W} + \frac{2(g_1 + h_1) \Gamma + [G \cdot \rho \pm H \cdot \rho S_Z]}{2[\Gamma^2 + \Gamma(g_2 + h_2) \rho + B \cdot \rho^2]}, \quad (14)$$

from here, we can find frequency difference between two component condensate as

$$\omega_+ - \omega_- = \frac{\Delta\tilde{\Omega} \cdot W}{\gamma_C}, \quad (15)$$

here,

$$\Delta\tilde{\Omega} = \tilde{\Omega}_+ - \tilde{\Omega}_- = \rho(\mathbf{r}_p) S_Z(\mathbf{r}_p) \{(\beta_1 - f_1)/W - (g_1 - h_1)(g_2 - h_2)/[\Gamma^2 + \Gamma(g_2 + h_2) \rho + A \rho^2]\},$$

here, we have defined condensate polarization $S_Z(\mathbf{r}_p) = |\zeta_+(\mathbf{r}_p)|^2 - |\zeta_-(\mathbf{r}_p)|^2$ and coefficient of density square term $B = (g_2 + h_2)^2(1 + S_Z^2)/4$, which has maximal value $(g_2 + h_2)^2/2$ for the total polarization ± 1 . Interestingly, we can see that energy gap is polarization $S_Z(\mathbf{r}_p)$ dependence and especially, which does not depend on the laser power when $\beta_1 \simeq f_1$ or large enough laser power.

Local condensate density wave vector $\mathbf{k}_C(\mathbf{r})$ is reaching maximal value with the condensate density decreased and spin polarized away from the pumping center. Polaritons condense at the laser spot position has a large blueshifted energy due to their interactions with uncondensed hot excitons, thus within a short time, these interaction energy will lead to the motion of polariton initially localized at pumping point. In particular, spontaneous polarization would happen because polarization may lower the frequency significantly under the laser power is large enough

as seen from Eq. 14, especially, spin domain, spin current and topological defect may be formed under appropriate condition.

In the following section, through extensive numerical simulations of the Eq. 1 coupled to the reservoir evolution Eq. 2, the robustness of above analytical considerations and, in particular, the dynamical formation of spin domain, spin current and half vortex for the typical values of the experimental parameters have been verified for a wide range of pump parameters.

V. NUMERICAL RESULTS FOR SPONTANEOUS POLARIZATION.

Equations can be solved numerically with the initial condition $n_{R\sigma}(x, y, t) \approx 0$, $\psi_{\sigma}(x, y, t) \approx 0$. The parameters of the pump are chosen in a way to compare with the experimentally observation [27, 27–29, 36] and condition. In our calculations we used the following parameters, typical for state-of-the-art GaAs-based microcavities: the polariton mass is set to $m = 10^{-4} m_e$ where m_e is the free electron mass. The decay rates are chosen as $\gamma_C = 0.152 \text{ ps}^{-1}$ and $\Gamma = 3.0\gamma_C$. The interaction strengths are set to $\hbar\beta_1 = 40 \mu\text{eV } \mu\text{m}^2$, $f_1 = -0.1\beta_1$, $g_1 = 2\beta_1$, $h_1 = -0.2\beta_1$, and condensation rate to $\hbar g_2 = 0.16 \text{ meV } \mu\text{m}^2$, $\hbar h_2 = 0.016 \text{ meV } \mu\text{m}^2$, and condensation loss rate $-\hbar\beta_2 = 0.16 \text{ meV } \mu\text{m}^2$, $\hbar f_2 = 0.016 \text{ meV } \mu\text{m}^2$. The pump intensity was chosen to match the experimentally measured blueshift of the polariton condensate, and pump profile is Gaussian shape:

$$W(\mathbf{r}) = \frac{w_0}{\pi w_1^2} \sum_{i=1}^n e^{-\frac{(x-x_i)^2 + (y-y_i)^2}{w_1^2}},$$

here, for a typical case, $w_1 = 1.0$, $|x_i| = |y_i| = 1.5$, and w_0 is tuned accordingly.

As expected, the dynamics of spinor condensate tends to a dynamically stable steady state with a spontaneously circular polarization under increasing laser power as shown in Fig. 1(b). Threshold laser power for spontaneously circular polarization is larger than that of starting condensation which can be understood from the Eqs. 5 and 6. The coherent polarized polaritons ballistically fly away from the laser spot due to their interactions converted into kinetic energy of coherent polariton. In particular, the circular polarization rapidly saturates with increasing the pumping power and may lead to an almost full polarization of spinor condensate [17–19]. Surprisingly, almost full circular polarization will finally change back to the linear polarization with further increasing the laser power (i.e., the density of condensate exceeding a threshold value). The quantum pressure terms (especially, spin-dependent pressure terms) in Eqs. 10 and 11 has to be taken into account to understand this polarization saturates and going back to the linear polarization. In Fig. 1(c), density profiles of incoherent hot exciton and polariton condensate represent linear and circular polarization, respectively, for one set of parameters chosen in the spontaneously circular polarization regime. As is shown, while unpolarized hot excitons experience a limited diffusion,

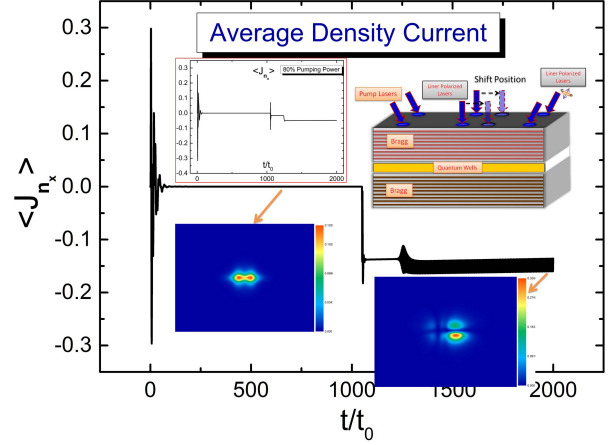


Figure 3: (Color online) Normalized average density current J_{n_x} of a coherent polariton condensate which is non-resonantly excited with 6 points linearly polarized laser. The insets shows the total density profile before and after shifting position of two linearly polarized lasers (see the schematic picture) along the x direction, and also shows J_{n_x} under decreasing the pumping power to 80%.

polarized polaritons ballistically fly away from the laser spot due to their interactions converted into kinetic energy of coherent polariton.

Fig. 2 show the density distribution of the calculated incoherent hot exciton and coherent polariton condensate for six and eight unpolarized pumping points, respectively. As is shown, while incoherent hot excitons experience a limited diffusion in such case, however, the neighbouring polarization of condensed polaritons are polarized with precisely opposite polarization determined by the density- and spin-dependent pressure terms. We shows the s_z distribution which clearly has the opposite circular polarization for two neighbouring site. This steady state is characterized by the magnetic domain wall formation corresponds to a vanishing total magnetization. As we have emphasized above that total effective external field is fundamentally generated and controlled by the spatial-dependent pump source which provide the coupling potential for the dynamics of particle density and spin density of exciton-polariton condensates. Thus, geometrical dependent interactions or geometrical effective magnetic field may lead to different and, perhaps, more complicated magnetic structures. Thus, in the following, we will study how to dynamically generate the spin current, fractionalized HQV and magnetic charge (or magnetic monopole) via dynamical tuning pumping (or geometrical) source.

VI. DENSITY CURRENT, SPIN CURRENT, TOPOLOGICAL CHARGE.

A. Density current

Physically, condensed fluid is a rather long-range cooperative phenomenon and is characterized by a special long-range correlation between the particles involving the coherent ordering of the momenta. The density-density, density-current and current-current correlation function

in some cases implies that the liquid has net surface currents and a net orbital angular momentum. It is therefore important to evaluate and generate the density current and spin current. We find that, by suddenly shifting a distance of pumping laser, the density and spin current can be dynamically generated, and integer vortices can be created as well. In particular, if shifted the pumping laser is circular polarized, fractionalized HQV can be successfully created which can be detected experimentally by means of polarization-resolved interferometry, real-space spectroscopy, and phase imaging technique [34].

To explain these features, we have performed simulations under a suddenly shifting the position of two middle pumping laser acting on polaritons. Fig. 3 gives an example of the outcome for a given realization of six linearly polarized pumping laser, and shows the normalized average polariton density current as function of time. As is shown in the Fig. 3, after switching on the pumping lasers, polariton experiences a large oscillation of density current within a short time, then, such density current oscillation decays very quickly and completely decreases to zero at 60 unit of time. The reason of large oscillation current in the early process is due to the large overlap of pumped hot exciton and polariton leading to the large repulsive force acting on the condensed polariton. However, with the diffusion of polariton under the repulsive force, a steady state with zero averaged current can be reached finally. Here, zero density current means polariton condensate reaches a balanced configuration in momentum space.

Next, in order to generate net density current, we suddenly shifting the two pumping lasers in the middle site at time 1050 (see the schematic picture of inset in the Fig. 3), a persistent current (about -0.15 in amplitude) with non-decay small oscillation is created successfully. Here, non-zero current can be understood as a new configuration in momentum space of condensed polariton after non-adiabatic modifying interaction energy between polariton and hot exciton by shifting pumping lasers. Especially, the small and fast oscillation in the density current can be understood as generating surface oscillation mode which is moved back and forth due to it's confined by the pumping laser. Interestingly, such surface oscillation mode can be suppressed completely by decreasing the pumping laser power (as is shown in the inset of Fig. 3, where pumping laser power has been decreased to 80 percent.). Fundamentally, generation of net surface currents can be thought as generating long-range density correlation in separated region by shifting a distance of the pumping lasers.

B. Spin current, topological defect.

In the strong coupling regime of semiconductor microcavities, due to their strong optical nonlinear response, spin polarization properties, and fast spin dynamics, polariton condensates are excellent candidates for designing novel spin-based devices. Here, we show the coherent transport of the spin vector of propagating polariton condensates. The observed nondissipative long-range spin transport is caused by exciting density-dependent effective

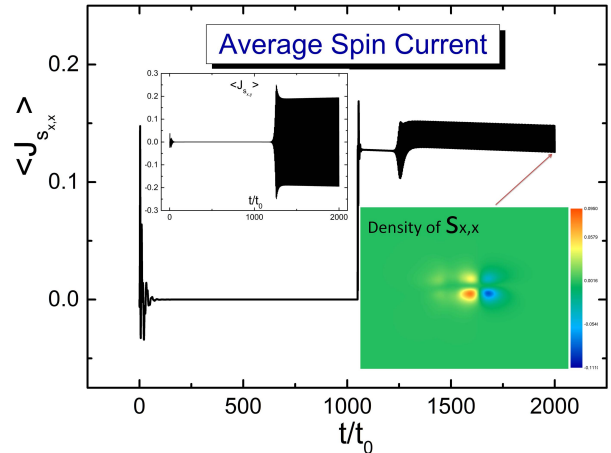


Figure 4: (Color online) Normalized average spin current $\langle J_{s,x} \rangle$ of a coherent polariton condensate which is non-resonantly excited with 6 points linearly polarized laser. The insets shows density profile of the spin current $J_{s,x,x}$ at the final stage after shifting position of two linearly polarized lasers along the x direction, and that for normalized average spin current along the y direction $\langle J_{s,y} \rangle$.

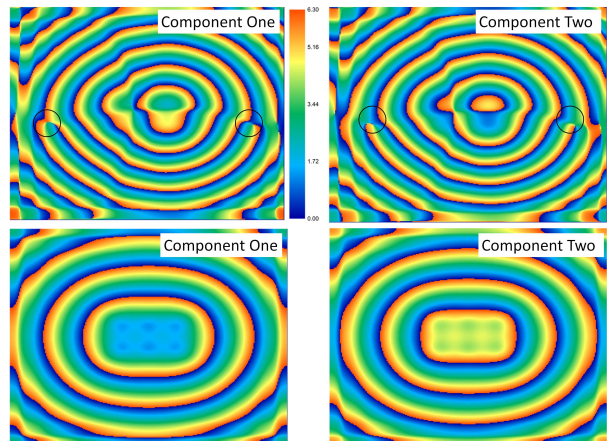


Figure 5: (Color online) Phase profile of each circular component of condensed polariton which is non-resonantly excited with 6 points linearly polarized laser. The up row and down row correspond to the phase map after and before shifting position of two linearly polarized lasers along the x direction, respectively.

magnetic field which can be utilized to generate polarization patterns as well as spin-polarized vortices.

Figure 4 shows average spin current $\langle J_{s,x} \rangle$ of a coherent polariton condensate as function of time which is non-resonantly excited with 6 points linearly polarized lasers. Similar to the behavior of average density current shown in Figures 3, persistent spin current is quickly developed after suddenly shifting the two pumping lasers in the middle site at time 1050. Here, the spin current is induced by the effective non-abelian gauge potential which is originated from spin-dependent interaction between hot exciton and coherent condensate. Similar to the Figure 3, the small and fast oscillation in the spin current is generated which can be understood as generating surface oscillation mode of spinor function due to it's confined by the pumping laser. Especially, average spin current moving along

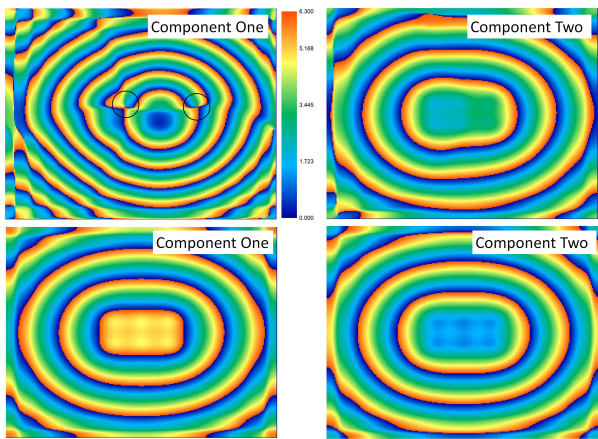


Figure 6: (Color online) Phase profile of each circular component of condensed polariton which is non-resonantly excited with 6 points linearly polarized laser. The up row and down row correspond to the phase map after and before shifting position of two linearly polarized lasers along the x direction, respectively.

the y direction $\langle J_{s,x,y} \rangle$ expects large oscillation across the zero value equally as is shown in the inset which means the stronger spin-dependent interaction and polarization reversed along the y direction with time evolution. The local spin current can be positive or negative value depending on the effective local gauge connection as is shown in the density of $s_{x,x}$.

Comparison to solid-state systems, the spatial-dependent pump sources inducing spin-dependent stimulation and dissipation for the condensed polariton provide a very promising way to generate and control the spin current and spin structure in the presence of different kinds of effective gauge fields (like Dresselhaus and Rashba fields), therefore open very broad possibilities for the studies of spinor quantum fluids and accessibility to their diverse quantum phases. In particular, such flexible and efficient way to control external pumping laser may generate fascinating topological defects dynamically which properties depend on the way how to manipulate the pumping laser.

Figures 5 shows the phase profile of each circular component of condensed polariton under shifting the linearly polarized lasers in the middle site. In such case, shifted laser is linearly polarized which means each circular component of condensed polariton experience a equally pumping source mainly originated from $V_R(\mathbf{r})$ in the Eq. 1. Thus, as expected, after some time evolution, the normal integer quantum vortex for each component has been generated and stable robustly as is shown in the upper row of 5 which is similar to the single component case [37, 38, 40, 41]. As is shown, two separated integer vortices with opposite circulation has been generated for each component, thus total angular momentum for each com-

ponent is still zero.

Now, the question is how to generate stable HQV in our studied system. In order to realize that, we now shift the position of one circularly polarized pumping lasers in the middle site (one linearly polarized laser is just the superposition of two circularly polarized lasers equally), and then see how the HQV is formed dynamically [32–36]. Very interestingly, steady exotic HQV can be successfully generated as is shown in 6 which has significant features that one component has vortices, but second component doesn't exist vortices. In particular, there are always two opposite circulation of HQV generated for one of component due to keep total angular momentum zero.

Generally, what kinds of stable topological defects are developed depending on the dynamics of gauge potential together with vector field, such as Maxwell-Chern-Simons-vector Higgs model for the superconductivity of Sr_2RuO_4 [46]. In our studied non-equilibrium exciton-polaritons liquid, incoherent hot exciton with pumping source and spin-dependent dissipation play important roles in topological excitation and make the dynamics of gauge potential more controllable comparing with conventional solid state system and ultracold atoms. HQV is analogous to the multicomponent quantum Hall system [73], which is the two-dimensional electron system in an external magnetic field violating parity and time reversal symmetry. Here we have mainly focused on dynamical creation of density, spin current and HQV induced by the effective non-abelian gauge potential at relatively short time; these phenomena can be conveniently probed by real-space spectroscopy, and phase imaging [34].

VII. CONCLUSIONS.

In conclusion, we have demonstrated a practical way to control spin polarization, induce density and spin current, and creating fractionalized vortices in exciton-polaritons semiconductor microcavities. For the polariton lifetime, the spin localization, spin polarization and exotic vortices can be readily excited in photoluminescence experiments and detectable by the time-resolved micro-photoluminescence spectroscopy [37, 74] or spin noise spectroscopy [75, 76]. Our results are of particular significance for creating these excitations in experiments and for exploring novel phenomena associated with them. This noticeably spin amplification and spin transport could offer a promising way to optimize spin signals in future devices with using polariton condensates.

We are grateful to N. Berloff for discussions. The financial support from the early development program of NanChang University and Skoltech-MIT Next Generation Program is gratefully acknowledged.

- [1] C. Weisbuch, M. Nishioka, A. Ishikawa and Y. Arakawa, Phys. Rev. Lett. **69**, 3314–3317 (1992).
- [2] A. Kavokin, J. Baumberg, G. Malpuech, F. Laussy. *Microcavities* (Oxford University Press, UK, 2011).

- [3] H. Deng, H. Haug, and Y. Yamamoto, Exciton-Polariton Bose-Einstein Condensation, Rev. Mod. Phys. **82**, 1489 (2010).
- [4] I. Carusotto and C. Ciuti, Rev. Mod. Phys. **85**, 299 (2013).

- [5] J. Kasprzak, M. Richard, S. Kundermann, A. Baas, P. Jeambrun, J. M. J. Keeling, F. M. Marchetti, M. H. Szymanska, R. André, J. L. Staehli, V. Savona, P. B. Littlewood, B. Deveaud, L. S. Dang, *Nature* **443**, 409 (2006).
- [6] H. Deng, G. Weihs, C. Santori, J. Bloch, and Y. Yamamoto, Condensation of Semiconductor Microcavity Exciton Polaritons, *Science* **298**, 199 (2002).
- [7] R. Balili, V. Hartwell, D. Snoke, L. Pfeiffer, and K. West, Bose-Einstein Condensation of Microcavity Polaritons in a Trap, *Science* **316**, 1007 (2007).
- [8] G. Christmann, R. Butté, E. Feltin, J.-F. Carlin, and N. Grandjean, *Appl. Phys. Lett.* **93**, 051102 (2008).
- [9] W. Xie, H. Dong, S. Zhang, L. Sun, W. Zhou, Y. Ling, J. Lu, X. Shen, and Z. Chen, *Phys. Rev. Lett.* **108**, 166401 (2012).
- [10] E. Wertz, L. Ferrier, D. D. Solnyshkov, R. Johne, D. Sanvitto, A. Lemaître, I. Sagnes, R. Grousson, A. V. Kavokin, P. Senellart, G. Malpuech, and J. Bloch, Spontaneous Formation and Optical Manipulation of Extended Polariton Condensates, *Nat. Phys.* **6**, 860 (2010).
- [11] C. Schneider, A. Rahimi-Iman, N. Y. Kim, J. Fischer, I. G. Savenko, M. Amthor, M. Lerner, A. Wolf, L. Worschech, V. D. Kulakovskii et al., An Electrically Pumped Polariton Laser, *Nature (London)* **497**, 348 (2013).
- [12] X. Lou, C. Adelmann, S. A. Crooker, E. S. Garlid, J. Zhang, K. S. M. Reddy, S. D. Flexner, C. J. Palmström, and P. A. Crowell, *Nat. Phys.* **3**, 197 (2007); M. Ciorga, A. Einwanger, U. Wurstbauer, D. Schuh, W. Wegscheider, and D. Weiss, *Phys. Rev. B* **79**, 165321 (2009).
- [13] S. P. Dash, S. Sharma, R. S. Patel, M. P. de Jong, and R. Jansen, *Nature (London)* **462**, 491 (2009); R. Jansen, *Nat. Mater.* **11**, 400 (2012).
- [14] S. Kéra-Cohen and S. R. Forrest, Room-Temperature Polariton Lasing in an Organic Single-Crystal Microcavity, *Nat. Photonics* **4**, 371 (2010).
- [15] D. Snoke, Spontaneous Bose Coherence of Excitons and Polaritons, *Science* **298**, 1368 (2002).
- [16] J. J. Baumberg, A. V. Kavokin, S. Christopoulos, A. J. D. Grundy, R. Butt, G. Christmann, D. D. Solnyshkov, G. Malpuech, G. Baldassarri Höger von Högersthal, E. Feltin, J. F. Carlin, and N. Grandjean, *Phys. Rev. Lett.* **101**, 136409 (2008).
- [17] H. Ohadi, A. Dreismann, Y. G. Rubo, F. Pinsker, Y. del Valle-Inclan Redondo, S. I. Tsintzos, Z. Hatzopoulos, P. G. Savvidis, and J. J. Baumberg, *Phys. Rev. X* **5**, 031002 (2015).
- [18] H. Ohadi, Y. del Valle-Inclan Redondo, A. Dreismann, Y. G. Rubo, F. Pinsker, S. I. Tsintzos, Z. Hatzopoulos, P. G. Savvidis, and J. J. Baumberg, *Phys. Rev. Lett.* **116**, 106403 (2016).
- [19] A. Askitopoulos, K. Kalinin, T. C. H. Liew, P. Cilibizzi, Z. Hatzopoulos, P. G. Savvidis, N. G. Berloff, and P. G. Lagoudakis, *Phys. Rev. B* **93**, 205307 (2016).
- [20] N. A. Gippius, I. A. Shelykh, D. D. Solnyshkov, S. S. Gavrilov, Y. G. Rubo, A. V. Kavokin, S. G. Tikhodeev, G. Malpuech, *Phys. Rev. Lett.* **98**, 236401 (2007).
- [21] T. K. Paraíso, M. Wouters, Y. Léger, F. Morier-Genoud, B. Deveaud-Pledran, *Nat. Mater.* **9**, 655 (2010).
- [22] C. Ouellet-Plamondon, G. Sallen, F. Morier-Genoud, D. Y. Oberli, M. T. Portella-Oberli, and B. Deveaud, *Phys. Rev. B* **93**, 085313 (2016).
- [23] A. Kavokin, G. Malpuech, M. Glazov, *Phys. Rev. Lett.* **95**, 136601 (2005).
- [24] C. Leyder, M. Romanelli, J. P. Karr, E. Giacobino, T. C. H. Liew, M. M. Glazov, A. V. Kavokin, G. Malpuech and A. Bramati, *Nat. Phys.* **3**, 628 (2007).
- [25] E. Kammann, T. C. H. Liew, H. Ohadi, P. Cilibizzi, P. Tsotsis, Z. Hatzopoulos, P. G. Savvidis, A. V. Kavokin, and P. G. Lagoudakis, *Phys. Rev. Lett.* **109**, 036404 (2012).
- [26] H. Flayac, D. D. Solnyshkov, I. A. Shelykh, and G. Malpuech, *Phys. Rev. Lett.* **110**, 016404 (2013).
- [27] A. V. Nalitov, G. Malpuech, H. Tercas, and D. D. Solnyshkov, *Phys. Rev. Lett.* **114**, 026803 (2015).
- [28] S. Dufferwiel, Feng Li, E. Cancellieri, L. Giriunas, A. A. P. Trichet, D. M. Whittaker, P. M. Walker, F. Fras, E. Clarke, J. M. Smith, M. S. Skolnick, and D. N. Krizhanovskii, *Phys. Rev. Lett.* **115**, 246401 (2015).
- [29] V. G. Sala, D. D. Solnyshkov, I. Carusotto, T. Jacqmin, A. Lemaître, H. Tercas, A. Nalitov, M. Abbarchi, E. Galopin, I. Sagnes, J. Bloch, G. Malpuech, and A. Amo, *Phys. Rev. X* **5**, 011034 (2015).
- [30] A. V. Nalitov, D. D. Solnyshkov, and G. Malpuech, *Phys. Rev. Lett.* **114**, 116401 (2015).
- [31] O. Bleu, D. D. Solnyshkov, and G. Malpuech, *Phys. Rev. B* **93**, 085438 (2016).
- [32] G. E. Volovik, *The Universe in a He-Droplet* (Oxford University Press, New York, 2003).
- [33] Y. G. Rubo, *Phys. Rev. Lett.* **99**, 106401 (2007).
- [34] K. G. Lagoudakis, T. Ostatnický, A. V. Kavokin, Y. G. Rubo, R. Andre, and B. Deveaud-Pledran, *Science* **326**, 974 (2009).
- [35] D. Sanvitto, F. M. Marchetti, M. H. Szymańska, G. Tosi, M. Baudisch, F. P. Laussy, D. N. Krizhanovskii, M. S. Skolnick, L. Marrucci, A. Lemaître, J. Bloch, C. Tejedor and L. Vina, *Nat. Phys.* **6**, 527 (2010).
- [36] R. Hivet, H. Flayac, D. D. Solnyshkov, D. Tanese, T. Boulier, D. Andreoli, E. Giacobino, J. Bloch, A. Bramati, G. Malpuech and A. Amo, *Nat. Phys.* **8**, 724 (2012).
- [37] K. G. Lagoudakis, M. Wouters, M. Richard, A. Baas, I. Carusotto, R. Andre, L. S. Dang and B. Deveaud-Pledran, *Nat Phys* **4**, 706 (2008).
- [38] G. Roumpos, M. D. Fraser, A. Löffler, S. Hofling, A. Forchel, and Y. Yamamoto, *Nat. Phys.* **7**, 129 (2011).
- [39] G. Nardin, G. Grosso, Y. Leger, B. Pietka, F. Morier-Genoud, and B. Deveaud-Pledran, *Nat. Phys.* **7**, 635 (2011).
- [40] D. Sanvitto, S. Pigeon, A. Amo, D. Ballarini, M. De Giorgi, I. Carusotto, R. Hivet, F. Pisanello, V. G. Sala, P. S. S. Guimaraes, R. Houdre, E. Giacobino, C. Ciuti, A. Bramati, and G. Gigli, *Nat. Photonics* **5**, 610 (2011).
- [41] T. Boulier, E. Cancellieri, N. D. Sangouard, Q. Glorieux, A. V. Kavokin, D. M. Whittaker, E. Giacobino, and A. Bramati, *Phys. Rev. Lett.* **116**, 116402 (2016).
- [42] D. J. Thouless, *Topological Quantum Numbers in Nonrelativistic Physics* (World Scientific, Singapore, 1998).
- [43] Anthony J. Leggett, *Rev. Mod. Phys.* **47**, 331 (1975); A. J. Leggett, *Modern Trends in the Theory of Condensed Matter*, Proceedings of the XVI Karpacz Winter School of Theoretical Physics (Springer, New York, 1980); A. J. Leggett (2006), *Quantum liquids: Bose condensation and Cooper pairing in condensed matter systems*, Oxford University Press, Oxford.
- [44] M. M. Salomaa and G. E. Volovik, *Rev. Mod. Phys.* **59**, 533 (1987).
- [45] D. Vollhardt and P. Wölfle, *The Superfluid Phases of Helium 3* (Taylor and Francis, London, 1990).
- [46] A. Mackenzie and Y. Maeno, *Rev. Mod. Phys.* **75**, 657 (2003).
- [47] T. L. Ho, *Phys. Rev. Lett.* **81**, 742 (1998).
- [48] T. Ohmi and K. Machida, *J. Phys. Soc. Jpn.* **67**, 1822 (1998).
- [49] F. Zhou, *Phys. Rev. Lett.* **87**, 080401 (2001).

- [50] S. Mukerjee, C. Xu, and J. E. Moore, Phys. Rev. Lett. **97**, 120406 (2006).
- [51] J. R. Kirtley, C. C. Tsuei, M. Rupp, J. Z. Sun, L. S. Yu-Jahnes, A. Gupta, M. B. Ketchen, K. A. Moler, and M. Bhushan, Phys. Rev. Lett. **76**, 1336–1339 (1996).
- [52] M. Yamashita, K. Izumina, A. Matsubara, Y. Sasaki, O. Ishikawa, T. Takagi, M. Kubota and T. Mizusaki, Phys. Rev. Lett. **101**, 025302 (2008).
- [53] J. Jang, D. G. Ferguson, V. Vakaryuk, R. Budakian, S. B. Chung, P. M. Goldbart and Y. Maeno, Science **331**, 186–188 (2011).
- [54] Jae-yoon Choi, Woo Jin Kwon, and Yong-il Shin, Phys. Rev. Lett. **108**, 035301 (2012).
- [55] Sang Won Seo, Seji Kang, Woo Jin Kwon, and Yong-il Shin, Phys. Rev. Lett. **115**, 015301 (2015).
- [56] G. Panzarini, L. C. Andreani, A. Armitage, D. Baxter, M. S. Skolnick, V. N. Astratov, J. S. Roberts, A. V. Kavokin, M. R. Vladimirova, and M. A. Kaliteevski, Phys. Rev. B **59**, 5082 (1999).
- [57] G. Dasbach, C. Diederichs, J. Tignon, C. Ciuti, P. Rousignol, C. Delalande, M. Bayer, and A. Forchel, Phys. Rev. B **71**, 161308 (2005).
- [58] M. J. Harris, S. T. Bramwell, D. F. McMorrow, T. Zeiske, and K.W. Godfrey, Phys. Rev. Lett. **79**, 2554 (1997).
- [59] C. Castelnovo, R. Moessner, and S. L. Sondhi, Nature (London) **451**, 42 (2007).
- [60] L. D. C. Jaubert and P. C.W. Holdsworth, Nat. Phys. **5**, 258 (2009).
- [61] T. Fennel, P. P. Deen, A. R. Wildes, K. Schmalzl, D. Prabhakaran, A. T. Boothroyd, R. J. Aldus, D. F. McMorrow, and S. T. Bramwell, Science **326**, 415 (2009).
- [62] D. J. P. Morris, D. A. Tennant, S. A. Grigera, B. Klemke, C. Castelnovo, R. Moessner, C. Czternasty, M. Meissner, K. C. Rule, J.-U. Hoffmann, K. Kiefer, S. Gerischer, D. Slobinsky, R. S. Perry, Science **326**, 411 (2009).
- [63] H. Kadowaki, N. Doi, Y. Aoki, Y. Tabata, T. J. Sato, J.W. Lynn, K. Matsuhira, and Z. Hiroi, J. Phys. Soc. Jpn. **78**, 103706 (2009).
- [64] S. T. Bramwell, S. R. Gibli, S. Calde, R. Aldus, D. Prabhakaran, and T. Fennell, Nature (London) **461**, 956 (2009).
- [65] S. S. P. Parkin, M. Hayashi, and L. Thomas, Science **320**, 190 (2008).
- [66] T. Busch and J. R. Anglin, Phys. Rev. A **60**, R2669 (1999).
- [67] H. T. C. Stoof, E. Vliegen and U. Al Khawaja, Phys. Rev. Lett. **87**, 120407 (2001).
- [68] M. H. Szymańska, J. Keeling, and P. B. Littlewood, Phys. Rev. Lett. **96**, 230602 (2006).
- [69] I. Carusotto and C. Ciuti, Phys. Rev. Lett. **93**, 166401 (2004).
- [70] M. Wouters and I. Carusotto, Phys. Rev. Lett. **99**, 140402 (2007).
- [71] M. Wouters, I. Carusotto, and C. Ciuti, Spatial and Spectral Shape of Inhomogeneous Nonequilibrium Exciton-Polariton Condensates, Phys. Rev. B **77**, 115340 (2008).
- [72] D. Porras, C. Ciuti, J. J. Baumberg, and C. Tejedor, Phys. Rev. B **66**, 085304 (2002).
- [73] S. M. Girvin, A. H. MacDonald, in Perspectives in Quantum Hall Effects, S. Das Sarma, A. Pinczuk, Eds. (Wiley, New York, 1997),
- [74] A. Amo, D. Sanvitto, F. P. Laussy, D. Ballarini, E. d. Valle, M. D. Martin, A. Lemaitre, J. Bloch, D. N. Krizhanovskii, M. S. Skolnick, C. Tejedor, L. Vina, Nature **457**, 291 (2009).
- [75] V. S. Zapasskii, Adv. Opt. Photon. **5**, 131 (2013).
- [76] J. Hübner, F. Berski, R. Dahbashi, M. Oestreich, Phys. Status Solidi (b) **251**, 1824 (2014).